EFFICIENT, HIGH BRIGHTNESS SOURCES OF POLARIZED NEUTRONS AND PHOTONS AND THEIR USES

J.E. SPENCER[a]
Stanford Linear Accelerator Center
Stanford University, Stanford, CA 94309, USA

There are many applications that could benefit from an easily accessible source of monochromatic, high brightness, polarized gammas and neutrons. A compact and comparatively inexpensive system is discussed based on a low-energy, electron storage ring with undulators that is expected to provide 10^{11} epithermal n/s and 10^{15} γ/s. This method could provide a more efficient, cleaner way to produce epithermal neutrons than conventional means. Technical innovations that make it feasible are described together with some fundamental and practical applications that also take advantage of developments in the field of high power lasers.

1 Introduction

Since Chadwick's discovery of the neutron (1932) and Szilard's patent on means for production (1935), there have been surprisingly few practical applications beyond their somewhat problematic use to produce power. For example, a presumably valid application was proposed within three months of Szilard's patent for what is now called Neutron Capture Therapy (NCT) that is still in the research stage[1]. Similarly, although research reactors have been around for some 50 years, they have been likened to a 'pig hunting for truffles'.

The system proposed here consists of a low energy storage ring with at least one undulator based oscillator. If the cavity length is any harmonic of the ring circumference ($L_C = \beta L_R n/n_B$ with n_B the number of bunches), higher-energy, secondary photons from Compton backscattering may be significant. Then, besides synchrotron radiation and undulator photons, there are also frequency upshifted Compton photons and photoneutrons from Be or D targets. While the primary electron energy depends on the application, higher energies are more versatile and technically much simpler but more expensive.

Practical applications for photons, well matched to 100 MeV electrons, include commercial, medical, materials and nuclear science applications based on photon energies up to 2-3 MeV – especially microlithography at 100-150 nm wavelengths and lower. Practical uses for neutrons include the real-time production of radioactive nuclides and other uses where there is no direct production of radioactivity e.g. the treatment of malignant and essentially inoperable brain tumors using NCT e.g. BNCT based on $^{10}B(n,\alpha)Li^7$.

[a]Work supported by the US Department of Energy, Contract DE-AC03-76SF00515.

Fundamental applications include studies of the QCD vacuum, neutron condensates and experiments[2] related to Grand Unification and cosmologic matter-antimatter asymmetries. Measurements of the neutron electric dipole moment using high power lasers or the neutron oscillation period $\tau_{n\bar{n}}$ ($n \to \bar{n} \to n$) in a baryon number violating process (ΔB=2) or lepton violating processes (ΔL=2) such as $nn \to ppe^-e^-$ are closely related and intriguing examples. These types of experiments require new tools and experimental knobs to control brightness, polarization, energy and time structure of the beams when *null* results are possible or expected to achieve quantifiable results.

2 The System

Figure 1 shows the key elements of a system that was developed in 1995[3] that is compact and comparatively inexpensive e.g. one that appears practical for university environments. The main element is an electron storage ring based on a practical, third-order, achromatic lattice. For 100 MeV electrons, an 8 mm wavelength undulator produces 11 eV polarized UV photons. These photons can be stored with high efficiency in a multimode oscillator cavity formed of multilayer Al, Mg (or Li) mirrors.[4] This cavity can be tuned to provide a Compton endpoint energy of 1.7 MeV. When incident on a Be conversion target these photons make epithermal neutrons strongly peaked near 25 keV from the $Be^9 + \gamma \to n + Be^8(\to 2\alpha)$ two-body reaction with negligible induced radioactivity.

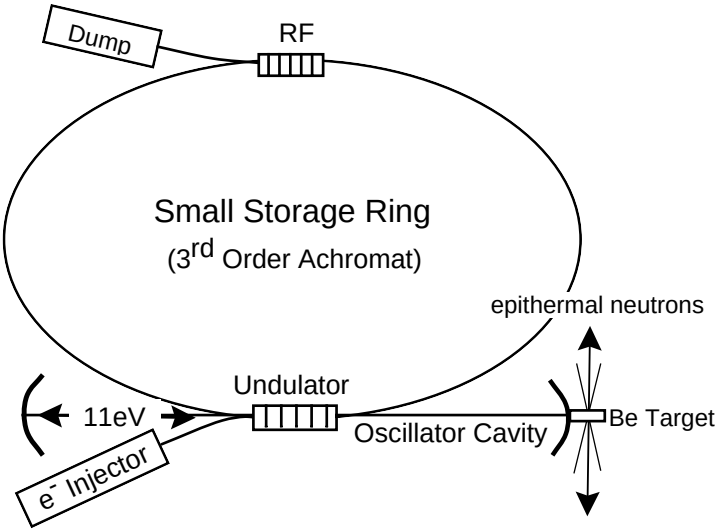

Fig. 1: Schematic layout of a compact photon and neutron source.

3 Considerations on Cost and Machine Configuration

Let's assume that both the cost and compactness of a ring can be taken as proportional to its circumference:

$$C = N_B L_B + N_Q L_Q + N_S L_S + N_O L_O + L_{Drift} + L_{RF} + L_{Undul.} + L_{Insert.}$$

where $N_B L_B = 2\pi\rho_B$. If the building costs go as the area, the overall facility cost will be proportional to $C(1 + aC/4\pi)$ where one expects $aC < 4\pi$. Ignoring the 'difficulty' costs to achieve full functionality, we want to minimize C. In the absence of other constraints, a combined function magnet eliminates most of the terms in C and a high-field superconductor minimizes the major remaining term $2\pi\rho_B$ and maximizes the critical synchrotron radiation energy $\mathcal{E}_c$ from

$$\rho_B[cm] \approx \frac{1}{3}\frac{\mathcal{E}_e[MeV]}{B[T]} \qquad \text{and} \qquad \mathcal{E}_c[keV] \approx \frac{2}{3}\mathcal{E}_e^2[GeV]B[T] \ .$$

Notice that it isn't especially difficult to get 11 eV photons at 100 MeV but the intensity required for Compton conversion is quite another question.

One obvious problem, especially for a superconducting system, is the space to accommodate other components such as the RF, injection and undulator insertions. Another involves getting adequate optics and field quality in higher order and the related question of tunability. Also, as one reduces ρ_B, the fractional energy spread increases according to [5]

$$\sigma_\varepsilon^2 = c_q \gamma^2 / \rho J_\varepsilon \quad \text{where} \quad c_q = 3.84 \cdot 10^{-13} \ m \ .$$

Because the dispersion η for a weak focusing magnet goes as $\rho/(1-n)$, the effective transverse spot size actually goes as $\sqrt{\rho}$ if the field index n is held constant. However, because the momentum compaction α is η/ρ so that $1 < \alpha < 4$, it follows that the increased energy spread gets magnified in the bunch length. Although the beam becomes unstable or antidamped for $0 \leftarrow n \rightarrow 0.75$, none of this is deadly unless the intensity or the monochromatic intensity is important. The solution is to change the optics by increasing the number of magnets to allow insertions but using a new type of combined function dipole.

4 Why Not Use a Synchrotron Radiation Source?

While simple, inexpensive, tabletop synchrotron radiation sources would be useful, especially for dedicated applications, their compactness limits their use e.g. they can't produce gammas and neutrons (excepting through the possible use of extremely intense and expensive lasers) in the form or with the intensities that are required.

The lowest energy SR source that we found was NIST's[b] Synchrotron Ultraviolet Radiation Facility II (SURF II) – a 300 MeV, weak-focusing ring having one superperiod based on the original synchrotron magnet having a field index $n = -\frac{\rho}{B}\frac{dB}{dx} = 0.59$ and central field B=1.2 T. The critical energy of synchrotron radiation is $\mathcal{E}_c$=71.8 eV. For a beam current of 200 mA over the flat, maximal part of the synchrotron light spectrum ($\omega \approx$5-25 eV) one expects

$$\frac{dN_{max}(\omega)}{d\theta dt} \approx 2.5 \cdot 10^{16} \mathrm{I}[A]\mathcal{E}_e[GeV]\frac{\delta\omega}{\omega}$$

for θ in milliradians. The integrated flux around the *full* SURF ring is then 10^{17} photons per second per 1% bandwidth or $1.5 \cdot 10^{13}$ photons/s/mr. This is clearly not enough even if we could use them all.

From the expressions above, the maximum 'brightness' doesn't change but only shifts upwards in photon energy with increasing field B for constant energy $\mathcal{E}_e$ and current I. However, at a LEP energy of 50 GeV and 20 mA, we get $\mathcal{E}_c \approx 1.7$B[T] MeV i.e. the secondary photons we need at 10 kG but only $2.5 \cdot 10^{14}$ photons/s/mr for 1 % bandwidth. This possibility as well as that of using one or more wiggler insertions to enhance the intensity was considered in 1980.[6] Thus, it is clear that we can't get the primary photon flux in the bandwidth we need without at least an undulator insertion and high Q oscillator cavity.

Besides allowing such insertions, other advantages of a small storage ring, aside from power usage, duty factor and natural emittance, compared to linacs, synchrotrons or recirculators is the radiation levels that are only high during injection. Thus, minimal shielding is required if humans are excluded during injection because there is comparably little charge involved to obtain high currents. Not only does each beam particle get used many times, it is used efficiently by using undulators matched to the specific application and the primary electron energy. We were unable to find any current system in the 50-200 MeV energy range that is considered reasonable for cost and compactness.

5 The Ring Lattice

Our first candidate lattice[3] superperiod is shown in Fig. 2. It has one family of C-dipoles, two quad, two sextupole and four octupole families – all with modest strengths. While longer than SURF, it has two long and fourteen short (0.8 m) insertions that account for most of the increased length. It is a practical, highly achromatic lattice that has comparably few multipole families. This implies that it can be operated as an FEL with significant gain enhancement depending on the dynamic aperture and damping that can be achieved.

[b] The characteristics given here were derived from information obtained from **nist.gov**.

Given a lattice, one can calculate the usual synchrotron radiation integrals that determine the unperturbed, equilibrium[5] damping times and emittances:

$$\epsilon_x \approx \frac{1}{2\pi}\frac{c_q\gamma^2}{\rho^2 J_x}\oint_D(\beta_x\eta_x'^2 + 2\alpha_x\eta_x\eta_x' + \gamma_x\eta_x^2)ds = \frac{1}{2\pi}\frac{J_\epsilon}{\rho J_x}\sigma_\epsilon^2\oint_D \mathcal{H}ds$$

where α_x=-$\beta_x'/2$ and γ_x=$(1+\alpha_x^2)/\beta_x$ and the other machine functions are given in Fig. 2. Using these for 100 MeV electrons gives:

$$\epsilon_{x,y} \approx 0.234\frac{\mathcal{E}_e^2[GeV]}{\rho^2}\oint_D \mathcal{H}ds\ [\mu\text{m}]\ =\ 0.057\mu\text{m}$$

because the damping partitions are $J_{x,y,\epsilon}$=1.005,1,1.995. This emittance is acceptable compared to $\lambda/4$ of the UV radiation and for single-turn injection. It can be improved by reducing η and β from their peak values in the lattice.

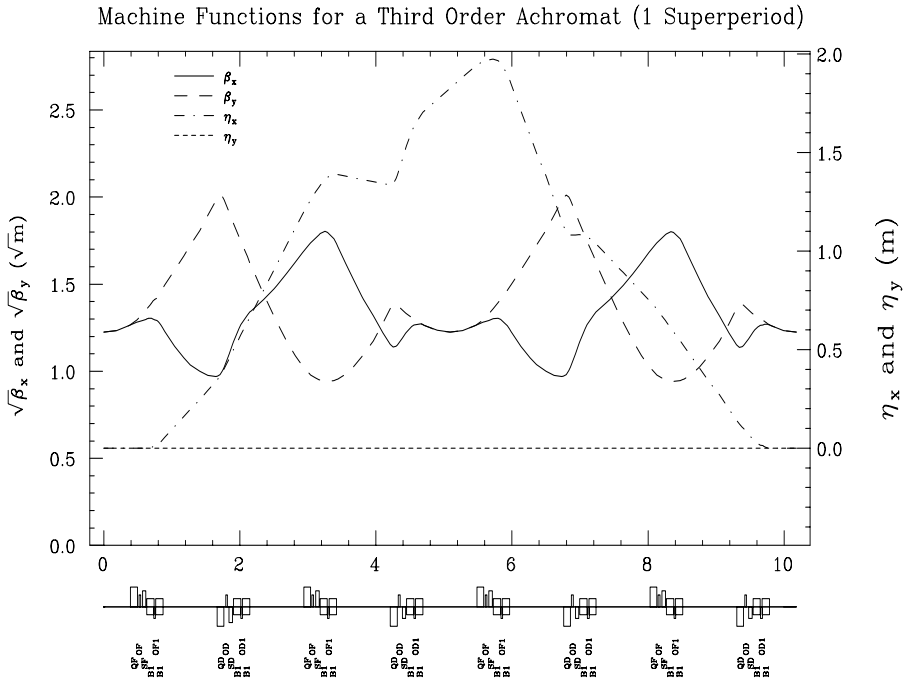

Fig. 2: Machine functions and magnetic components for one superperiod.

With ϵ_x=ϵ_y=0.057 μ for the electron beam and β_x=β_y=1.5 m from Fig. 2 at the insertion waist where η_x=η_y=0 gives equilibrium RMS parameters:

$\epsilon_{x,y} = 0.057\ \mu\text{m}, \quad \beta_{x,y} = 1.5\ \text{m} \quad \Rightarrow\ \sigma_{x,y} = 0.29\ \text{mm},\ \sigma_{x',y'} = 0.20\ \text{mrad}$

in the undulator. By design, these angles are less than the characteristic $1/\gamma$ divergence of the radiation to preserve Compton energy-angle correlations. While *not* maximized for a minimal spot, they do not lead to any significant increase in the natural (SR) emittance when there is fast damping.

6 Other RF and Lattice Constraints

We want a small synchrotron tune ν_s and a large R_{56} from the Compton source to the RF cavities to restore the large energy loss so that the producing electron in the secondary process is not lost before it damps enough to make another photoneutron. If $\mathcal{E}_C$ is the secondary Compton photon energy, we have:

$$R_{56}(s_1 \to s_2) = \int_{s_1}^{s_2} \frac{\eta_x(s)}{\rho(s)} ds \gg \frac{\sigma_z}{\delta_C} \quad \text{when } s_1 = z_{undul},\ s_2 = z_{RF}, \delta_C = \mathcal{E}_C/\mathcal{E}_e\ .$$

This is equivalent to the momentum compaction α when the integral is taken around the ring. We note that R_{56} is cumulative around the superperiod, being a maximum at the end but for high gain FEL action we want $\alpha\delta\mathcal{E}_e/\mathcal{E}_e \ll \lambda/\beta cT$ where λ is the FEL wavelength and T is the ring period.

A value for ν_s=0.1 implies one can replace as much of the lost energy as V_{RF} and R_{56} allow for a given RF frequency:

$$\delta\mathcal{E}_e = eV_{RF}\sin(2\pi R_{56}\mathcal{E}_C/\mathcal{E}_e\lambda_{RF})\ .$$

For R_{56}=-2.83 cm/% and V_{RF}=2 MV we see that 1.37 MeV is regained or about 80 % of the energy is restored on the first pass through the RF when we use a frequency of f=750 MHz (λ_{RF}=40 cm). It also implies several orders of magnitude gain is possible for the primary photon intensity in FEL mode.

$\delta\mathcal{E}_e$ varies nearly linearly with R_{56}, $\mathcal{E}_C/\mathcal{E}_e$, f_{RF} and V_{RF} which gives at least three alternatives – all with different cost implications. One can increase V_{RF}, R_{56} or f by themselves or in combination. Increasing f decreases single bunch instabilities by allowing lower bunch charges but decreases bunch length and potentially the bunch lifetime via intrabeam scattering. However, turbulent bunch lengthening sets in at currents on the order of a few milliamps/bunch if not counteracted[7] by FEL bunching. The natural bunch length is $\sigma_l \approx 1$ mm or so - depending on V_{RF} and the tune is $\nu_s \approx 0.1$.

Beyond the incoherent energy loss from SR, the losses from resistive wall (Cu or glidcop) and parasitic modes are typically only 45 eV/turn giving a combined total of <250 eV/turn/particle. With a current of 1 A, this implies an average power of only 0.25 kW, ignoring any RF inefficiencies, primary (coherent) FEL or secondary Compton damping (dominant at 26 keV/turn).

7 The Primary Photon Energy $\mathcal{E}_{\gamma 1}$ and Intensity

We will use a planar helical undulator to produce polarized UV photons to produce Compton photons having an endpoint energy $\mathcal{E}_{\gamma 2}^{max} \equiv \mathcal{E}_C$=1.7 MeV. These, in turn, can be used to produce epithermal neutrons having kinetic energies peaked near 25 keV. This is a good range for BNCT on inoperable brain tumors but can be decreased or moderated. The primary photon energy from the undulator is:

$$\mathcal{E}_{\gamma 1}(\theta) = \frac{2\gamma^2}{(1+\gamma^2\theta^2+\frac{1}{2}\mathrm{K}^2)}(\frac{hc}{\lambda_u})$$

where θ is the radiation angle in the plane of the undulation. This relation for the angular dependence is valid for $\sigma_{x'}=\sigma_{y'} \ll 1/\gamma$. The peak energy is

$$\mathcal{E}_{\gamma 1}^{max}[eV] = \frac{2\gamma^2}{(1+\frac{1}{2}\mathrm{K}^2)}(\frac{hc}{\lambda_u}) = \frac{949.6}{(1+\frac{1}{2}\mathrm{K}^2)}\frac{\mathcal{E}_e^2[GeV]}{\lambda_u[cm]}$$

and the photon flux at the peak energy is

$$\frac{dN_{max}(\mathcal{E}_{\gamma 1}^{max})}{dt} \approx 1.4 \cdot 10^{17} \frac{\mathrm{N}_u \mathrm{K}^2 \mathrm{I}[A]}{(1+\frac{1}{2}\mathrm{K}^2)} \frac{\delta\omega}{\omega}$$

where N_u is the number of periods and B_u, λ_u and K are related in the usual energy independent way:

$$\mathrm{K} = e\mathrm{B}_u/mck_u = 0.934\mathrm{B}_u[\mathrm{T}]\lambda_u[cm] \ .$$

K defines the maximum angle (K/γ) between the electron's velocity in the undulator and the longitudinal axis whenever the rms beam divergence is much smaller. As noted above, this will always be the case because $N_{max} \rightarrow 0$ as K^2.

With $\mathrm{B}_u^2 = \mathrm{B}_x^2 + \mathrm{B}_y^2$ in this definition of K, the expressions for $\mathcal{E}_{\gamma 1}$ and $\dot{N}$ apply for both helical and planar undulator types in lowest order and for small enough K when we also make the replacement $\mathrm{K}^2 = K_x^2 + K_y^2$. At 100 MeV, this implies that B_p=7.17 and B_h=5.07 kG for the same flux of photons. Both types of undulators appear feasable with these particular fields.

Using $\mathrm{N}_u \geq 40$ provides a Compton endpoint energy $\mathcal{E}_C^{max} \geq \mathcal{E}_{T_n}$=1.66 MeV whereas $\mathrm{N}_u = 2\beta_{x,y}/\lambda_u$=400 is an optimum match to the 1.5 m beta function at the undulator. Using N_u=200 with an average current of 1 Amp gives an integrated flux of $1.5 \cdot 10^{17}$ photons per second produced in the bandwidth of the undulator's fundamental that can produce a Compton endpoint energy from 1.66-1.70 MeV (see next section). For 75 bunches and 10^7 turns this is only $2 \cdot 10^8$ photons/pass/bunch. With no gain and good mirrors this gives intracavity pulses $N_{\gamma 1} \geq 10^{11}$ at 10 kHz i.e. with ring down times τ_Q=0.1 ms.

8 The Secondary Photon Energy $\mathcal{E}_{\gamma 2}$ and Intensity

Compton Scattering as an eγ conversion and frequency upshifting technique can occur in many ways, e.g., in wigglers, undulators and FELs, the initial photons are the low frequency, virtual components of static fields. Ordinary, single-photon CS (order $r_{\rm e}^2$), in terms of relativistic invariants, is

$$\frac{d\sigma}{dy} = \frac{2\pi r_{\rm e}^2}{x}\left[(1-y) + \frac{1}{(1-y)} - \frac{4y}{x(1-y)} + \frac{4y^2}{x^2(1-y^2)} + 2\sigma_{\rm e,e'}\lambda_{\gamma,\gamma'}F_{\rm P}\right]$$

where $4\pi r_{\rm e}^2 \approx 1$ barn, with the helicities $\sigma_{\rm e,e'} = \pm\frac{1}{2}, \lambda_{\gamma,\gamma'} = \pm 1$ and

$$F_{\rm P} = \frac{y}{(1-y)}(2-y)\left[1 - \frac{2y}{x(1-y)}\right] \ .$$

The relativistic invariants are

$$x = \frac{s}{p\cdot p} - 1 = \frac{2p_1\cdot k_1}{p_1\cdot p_1} = 2\frac{\mathcal{E}_1\mathcal{E}_{\gamma 1}}{m^2}(1+\beta\cos\theta_1) \leq \ 0.0153\,\mathcal{E}_1[\mathrm{GeV}]\,\mathcal{E}_{\gamma 1}[\mathrm{eV}]$$

where $\theta_1 = 0$ defines head-on scattering (in the lab) and

$$y = 1 - \frac{u}{p\cdot p} = \frac{2p_1\cdot k_2}{p_1\cdot p_1} = \frac{2\mathcal{E}_1\mathcal{E}_{\gamma 2}}{m^2}(1-\beta\cos\theta_2) = \frac{\mathcal{E}_{\gamma 2}}{\mathcal{E}_1} \ + \ \mathcal{O}({\theta_2}^2)$$

Integration gives the total cross section $\sigma_C = \sigma_{\rm NP} + 2\sigma_{\rm e,e'}\lambda_{\gamma,\gamma'}\sigma_{\rm P}$ where

$$\sigma_{\rm NP} = \frac{2\pi r_{\rm e}^2}{x}\left[\left(1 - \frac{4}{x} - \frac{8}{x^2}\right)\ln(1+x) + \frac{1}{2} + \frac{8}{x} - \frac{1}{2(1+x)^2}\right] \rightarrow \frac{2\pi r_e^2}{x}(\ln x + \frac{1}{2})$$

$$\sigma_{\rm P} = \frac{2\pi r_{\rm e}^2}{x}\left[\left(1 + \frac{2}{x}\right)\ln(1+x) - \frac{5}{2} + \frac{1}{1+x} - \frac{1}{2(1+x)^2}\right] \rightarrow \frac{2\pi r_{\rm e}^2}{x}(\ln x - \frac{5}{2})$$

The arrows give the ultrarelativistic case, $x \gg 1$. For an electron at rest in the lab ($x = 2\omega/m$), $\sigma_{\rm NP}$ and $\sigma_{\rm P}$ both fall rapidly compared to the Thomson limit for $x > 1$. For $x \ll 1$, $\sigma_{\rm NP} = 8\pi r_{\rm e}^2(1-x)/3$, the Thomson result. The total cross section typically depends less on the polarization than does the outgoing photon energy distribution. For example, $\sigma_{\rm P} = 0$ for $x = 2.5$, but for $y = 0.7$ near $y_{\rm max} = x/(1+x)$, the spectrum can differ by a factor of six. Some characteristic distributions for $\mathcal{E}_{\gamma 1}$=1.17, 2.8 and 11.1 eV at 100 MeV were given[3] previously and in more detail[8] elsewhere.

For small θ_1 and $\mathcal{E}_{\gamma 1}$, the secondary Compton photon energy is:

$$\mathcal{E}_{\gamma 2}(\theta_2) = \frac{4\gamma_1^2}{(1+\gamma_1^2\theta_2^2 + 4\gamma_1\mathcal{E}_{\gamma 1}/mc^2)}\mathcal{E}_{\gamma 1}$$

We can make the correspondence $\mathrm{K}_C^2=8\gamma\mathcal{E}_{\gamma 1}/mc^2\ll 1$ for most $\mathcal{E}_1=\mathcal{E}_e$ and $\mathcal{E}_{\gamma 1}$:

$$\frac{1}{2}\mathrm{K}_C^2 = 0.0153\mathcal{E}_e[GeV]\mathcal{E}_{\gamma 1}[eV] \ .$$

For the example at 100 MeV, K_C=0.186. $\mathcal{E}_{\gamma 1}$ can be increased in several ways. For higher energies e.g. $\mathcal{E}_e$=200 MeV we could use a laser. While this is more expensive, the 'difficulty' costs probably favor it. Because the accelerator is expensive we would like to use lower energies to *simultaneously* allow the 0.11 μm microlithography option. The RMS addition to the electron beam's angular divergences given in Section 5 ($\sigma_{x'}=\sigma_{y'}$=0.20 mr) from the Compton process is negligible[3] because ψ_{e2}^{max}<0.003°≈50 μrad.

For gaussian incident bunches, the luminosity for $(e_1\vec{\gamma}_1 \rightarrow e_2\vec{\gamma}_2)$ reactions in terms of the particles in a single electron bunch N_B and the undisrupted, rms spot sizes $\sigma_{x,y}^*$ at the insertion is

$$\mathcal{L} \ = \ n_c\frac{n_t n_B N_B N_{\gamma 1} H_D}{4\pi\sigma_x^*\sigma_y^*}\zeta \ \rightarrow \ n_c\frac{n_t n_B N_B N_{\gamma 1}}{4\pi\widehat{\sigma}^2}\ \zeta \ = \ n_c\frac{I_e(A)}{e}(\frac{\mathcal{N}_{\gamma 1}}{4\pi\widehat{\sigma}^2})$$

where n_B is the number of bunches in the ring and n_t is the number of turns/s. $N_{\gamma 1}$ is the number of (incoherent) undulator photons/bunch from Sect. 7 and n_c is the number of collisions in the cavity a bunch makes in a single pass. The dimensionless parameter $\mathrm{H_D}$ defines the effective spot sizes in interaction and the arrow implies round spots with:

$$\sigma_{x,y}^* \equiv [\sigma_{x,y}^2+\lambda_{\gamma 1}\lambda_u \mathrm{N}_u/(4\pi)^2]^{\frac{1}{2}} \approx \sigma_{x,y} \approx \widehat{\sigma} \ .$$

$\mathcal{N}_{\gamma 1}$ is the effective number of photons per bunch in collision with single pass gain G and mirror efficiency R. For no gain or external sources ζ=1/(1-R^2).

Assuming mirrors with good reflection efficiency[4] R=0.999 and no gain gives $\mathcal{N}_{\gamma 1}=10^{11}$. Taking n_c=6 in the *multimode* cavity (or photon storage ring) gives $\mathcal{L}=3.6\cdot 10^{32}/\mathrm{cm}^2\mathrm{s}$. The reaction rate for Compton photons is then:

$$R_{\gamma 2} = \mathcal{L}\sigma_T = 3.6\cdot 10^{32}(\frac{2}{3}\cdot 10^{-24}) = 2.4\cdot 10^8 \ s^{-1}.$$

While this is comparably[9] quite good, it includes the full Compton spectrum.

One major limit is the ≈1J/cm^2/pulse threshold for mirror damage. For $\mathcal{E}_{\gamma 1}$=11.1 eV, $\lambda_{\gamma 1}$=112 nm

$$\sigma_{\gamma 1'} = \sqrt{\frac{\lambda_{\gamma 1}}{N_u\lambda_u}} \ \geq \ 0.2mr$$

for N_u≤400 which is the matching condition for $\beta_{x,y}$=1.5 m. Using N_u=200 gives an approximate 1 cm^2 spot. An RF frequency of f=750 MHZ (25 MW klystrons are commercially available) allows 75 bunches with $\mathcal{N}_{\gamma 1}^{max}\approx 6\cdot 10^{17}$ and $\mathrm{R}_{\gamma 2}=1.3\cdot 10^{15}$/s or $\mathrm{R}_{\gamma 2}=1.3\cdot 10^{13}\delta_{\gamma 2}(\%)$ where $\delta_{\gamma 2}=\delta\mathcal{E}_{\gamma 2}/\mathcal{E}_{\gamma 2}$. From the Madey gain-spread theorem, this appears impossible at this frequency without including an external assist[10] e.g. from the injector or conventional laser.

9 Neutron Production

The first use of ^{9}Be photodisintegration was by Szilard and Chalmers (1934) using a radium γ source. Under our assumptions, we had $\zeta_{\gamma 2} \leq 0.04/1.7 = 2.4$ % of the Compton photons capable of producing neutrons of which 0.3 % are expected to make neutrons[11] before Compton scattering or absorption[12] so that $\zeta_n \leq 7.2 \cdot 10^{-5}$. This translates into a monochromatic neutron rate $R_n = 10^{11}$ n/s with mean energy $\mathcal{E} = 24.8$ keV and $\sigma_{\mathcal{E}} = 6.8$ keV. This is easily improved, e.g.

1. Adding deuterium to the conversion target and increasing $\mathcal{E}_{\gamma 2} \geq 2.5$ MeV ($\mathcal{E}^D_{T_n} = 2.22$ MeV) increases the efficiency to $\zeta_{\gamma 2} \leq 34\%$ and $R_n = 1.4 \cdot 10^{12}$ n/s. Targets should use the energy-angle correlation in the $\mathcal{E}_{\gamma 2}$ spectrum.

2. Increasing the number of bunches via the RF frequency or circumference increases $\mathcal{L}$. The former is preferred for: 1) cost, 2) single bunch instabilities, 3) current and 4) better matching to the injector.

3. Increasing the electron energy allows more bunches having a higher N_B, $N_{\gamma 1}$ and $\mathcal{N}_{\gamma 1}$ because it allows higher efficiency mirrors, higher power lasers and faster damping but it also increases costs.

4. Using an existing ring e.g. PEP-II[13] that is well matched to the conditions with $I_e > 1$ A. Together with items (1 & 3) one expects $R_n > 10^{14}$ n/s.

The most important, competing atomic process over the extended energy range up to $\mathcal{E}_{\gamma 2} = 1$ MeV or more is Compton scattering which slowly moderates the incident photons. Thus, while ζ_n varies with $\mathcal{E}_{\gamma 2}$ and conversion target, it effectively increases which is a good reason to increase the photon energy. Conservatively, we have held ζ_n constant at 0.003 because this is also dependent on target geometry.

The best way to increase $\mathcal{E}_{\gamma 2}$ is to raise $\mathcal{E}_e$ to 121 MeV for $\mathcal{E}_{\gamma 1} = 11.1$ eV. This increases energy spread but ignoring Fermi motion there is still an energy-angle correlation that can be used in a neutron horn. Similarly, the BeD target should take advantage of the position-energy correlation in the $\mathcal{E}_{\gamma 2}$ Compton spectrum. If moderation is required, D_2O can be used to produce and moderate because the (n,p) cross section is quite large[12] (1.6 barns/sr) and rather flat.

Assuming $R_n = 1.4 \cdot 10^{12}$ n/s for an average power of 26 kW to maintain the beam, we have $5.4 \cdot 10^{10}$ n/s/kW. For comparison, the thick target yield of photoneutrons produced by 100 MeV electrons on Be is $\approx 2.3 \cdot 10^{11}$ n/s/kW and $2.3 \cdot 10^{12}$ n/s/kW for tungsten spread over more than 50 MeV. Similarly, 1 kW of 1 GeV protons on high Z targets gives ≈ 25 $n/proton$ for a yield of $1.5 \cdot 10^{14}$ n/s/kW spread over a larger energy range. Thus, we appear to provide a cleaner, brighter, low-energy spectrum but with lower intensity.

Polarized neutrons are available by using circularly polarized photons. From the known, low-lying spin states of ^{9}Be, only dipole transitions are important. The ^{9}Be$(3/2^-)$ ground state has a magnetic moment dominated by the loosely bound neutron and the electric field of the incident photon induces an electric dipole moment from displacement of Be^8 from the center of mass. The interaction Hamiltonian between the field and nucleons is:

$$H_{N\gamma} = -\frac{e}{c}\sum \vec{j}_i \cdot \vec{A}(\vec{r}_i, t) \ .$$

The total cross section is proportional to the sum of squares of the matrix elements over the available state space:

$$\sigma(\gamma, n) = 4\pi^2 \frac{\omega}{c} \sum |M|^2 \ .$$

For low energies, well below that of the ^{9}Be$(5/2^+)$ excited state, one expects the electric dipole term to excite ^{9}Be$(1/2^+)$ that decays by s-wave neutron emission to ^{8}Be(0^+) with a reasonably flat cross section[11] up to 1.7 MeV. The width $\Gamma_{1/2^+}$ is 217 keV i.e. from threshold to 1.8 MeV while the next excited state at 2.43 MeV has $\Gamma_{5/2^-}$=80 keV. With quantization axis along $k_{\gamma 2}$ and $\mathcal{E}_{\gamma 2}$<2 MeV or so, one easily finds[8] $\mathcal{P}_{\rm RHC}(\vec{n})$=-0.5, $\mathcal{P}_{\rm LHC}(\vec{n})$=0.5, but with reduced flux, and $\mathcal{P}_{\rm Lin}(\vec{n})$=0. Circularly polarized photons above 2.5 MeV increase the polarized neutrons around 90° to the photon direction. This increases the overall efficiency by reducing atomic absorption and also increases $\zeta_{\gamma 2}$.

10 Practical Applications

^{10}B(n,α)Li^7, ^{6}Li(n,α)H^3 and ^{3}He(n,p)H^3 are all exothermic reactions having Q=2.78, 4.78, 0.76 MeV with large cross sections σ=3.84, 0.94, 5.33 kb. All of these materials have been used for neutron detection although only the first two are easily available. The (γ, n) reactions such as ^{9}Be(γ, n)Be^8 are endothermic where Q=-S$_n$=-1.66 MeV is the neutron separation energy. A (γ, α) reaction such as ^{7}Li(γ, α)H^3 has Q=-2.46 so there are several ways to make tritium that will be discussed. Similarly, there are several (n, γ) reactions that are exothermic that could be used to boost and pump $\mathcal{E}_{\gamma 2}$.

Some reactions that can be reversed to make neutrons are: ^{7}Li(α, n)B^{10}, ^{2}H(d, n)He^3, ^{7}Li(d, n)2He^4 or ^{7}Li(p, n)Be^7.The (d, n) reactions have positive Q values and 50 mb cross sections. Szilard and Chalmer's Ra-Be source made 0.8 MeV neutrons from the (γ, n) and >5 MeV from the ^{9}Be(α, n) reaction. They demonstrated a practical means of isotope production *and* separation using ethyl iodide (I^{127}) to produce medically useful I^{128}(T$_{1/2}$=0.4 hr).

Interest in BNCT or an equivalent is based on the ≈0.003% probability of a lethal brain tumor (predominantly high-grade gliomas) per annum. It uses the ^{10}B(n,α)Li^7 reaction with its large cross section to distribute the 2.8 MeV

of energy between short ranged (<10 μm) Li and α. Photon activation therapy (PAT) and related variants to NCT are associated reactions for electrons.

Tritium production from ^{7}Li(γ,α)H^3 is an interesting, nonmedical example of 'clean' radioactivity.Although monochromatic photons aren't needed, this method could still be cleaner and more efficient than bremsstrahlung.[15] We estimate, using σ_T=0.4 mb, that:

$$R_T = \zeta_\alpha \zeta_{\gamma 2} R_{\gamma 2} \cdot \sigma_T \cdot \rho_{Li} L_{Li} N_A / A_{Li} \approx 21 \text{ mg/year}$$

where $\zeta_\alpha\zeta_{\gamma 2}\approx$0.38 assuming a 10 MeV Compton endpoint, $L_{Li}=1/\mu_{pair}$ and $N_A=6{\cdot}10^{23}$. Similarly, the LER and HER rings at PEP-II would give 3 g/year.

Another important application that meshs well with the others at 100 MeV is microlithography at 0.11 μm or lower. This was the only reason, other than cost, for choosing 100 MeV even though the 'difficulty' costs are unquestionably higher. The theoretical limit,[7,10] based on the cavity ring down time of $2Q(L_C/c)\approx$0.1 ms, is 1 J/bunch at a 10 kHz rate. Unfortunately, the availability and lifetime of the mirrors makes this impractical at present.[10]

Such systems are not limited to one particular form of cancer therapy or other clinical possibilities using either neutrons or photons by themselves or in combination. The same can be said for the study of materials and fabrication techniques. Assuming that every type and scale of matter has a clear and unique signature, what we need are versatile sources. Known applications and the potential for others is so broad that no more needs to be said except to compare to the growth and costs of SR facilities.

11 Fundamental Processes

The dipole moments of the nucleon are not well understood even though the magnetic dipole moments of both the neutron and proton are well known. For *any* nondegenerate state of pure parity, the electric dipole moment (EDM) should be zero. However, because the neutron decays weakly via beta decay it is an interesting example to study. Further, because one expects to measure μ_E through its interaction with an electric field via $\mu_E\vec{\sigma}{\cdot}\vec{E}$ which is odd under both P and T but even under C, this violates P, CP and T. It therefore provides additional insight into the basic mechanism of T violation.

Because μ_E is presumably odd under C, the EDM of the antinucleon changes sign as does the magnetic moment relative to the nucleon. To date, a limit of $\mu_E<10^{-25}$ e-cm exists[16] for the neutron. Most measurements have used fields whose strengths have to be inferred from a model e.g. using the nuclear electric field implies a screening correction. We know of no attempt to use high power lasers for this measurement but a number of possibilities suggest themselves whenever one has both high power lasers and polarized neutrons.

Using a split, gaussian laser beam, one expects a paraxial, on-axis laser field (either electric or magnetic):

$$\mathcal{F}_z \approx -\sqrt{\frac{\eta_V P_L}{\pi}}\frac{4\theta w_\circ}{w^2}\exp\left(\frac{z^2\theta^2}{w^2}\right) \times \exp i\psi$$

where η_V is the vacuum wave impedance, P_L is the laser power and ψ is made of three phases.[17] To obtain net acceleration or field integral, it follows that there must be at least *one* boundary to terminate the field at $|z|<Z_R$. If $w_\circ$ is the waist size and $Z_R=\pi w_\circ^2/\lambda$ is the Rayleigh range, then the distribution that we have to match to the particle beam is:

$$w^2 = w_\circ^2[1+(\frac{z^2}{Z_R^2})] \ .$$

Electric fields on the order of 10^{10} V/m should be possible. With variable polarization, one can switch between the electric and magnetic coupling to calibrate against the expected rate from the magnetic moment.

Ignoring strangeness[c] (or hypercharge), the relation between a particle's charge Q, in units of e, its isospin and its baryon number is

$$\mathrm{Q} = \mathrm{I_3} + \frac{\mathrm{B}}{2} \ \rightarrow \ \mathrm{I_{3L}} + \mathrm{I_{3R}} + \frac{\mathrm{B-L}}{2}$$

where B=1, 0, -1 for nucleons, mesons and antinucleons and L=1, 0, -1 for leptons, hadrons and antileptons. At present, both Q, B and L are absolutely conserved i.e. there is no evidence that $\Sigma \mathrm{Q}_i$, $\Sigma \mathrm{B}_i$ and $\Sigma \mathrm{L}_i$ change in any interaction between known particles or groups of particles.

If charge is conserved, then the electron should be stable because there are no known lower energy charged particles. While there are no known reasons why lepton number should be conserved, there are no violations up to current energies. Similarly, the proton is stable because of the phenomenologically conserved baryon number. The neutron is stable in nuclei for similar reasons i.e. there are no allowed, lower energy states available. So why does one expect such effects? First, the Standard Model predicts both baryon and lepton nonconserving reactions but conserves B-L which appears to be the more general, global symmetry.[2] Second, and as important as life itself, cosmology implies a strong and locally obvious matter-antimatter asymmetry.

If lepton number is violated then neutrino oscillations are possible i.e. ΔL=2 occurs and by implication one then expects the ΔB=2 neutron process.

[c]The neutron has strangeness S=0 or hypercharge $\mathcal{Y}$=S+B=1. See Ref. 2 on the subject of the left-right symmetric, weak analog of the Gell-mann-Nishijima formula.

This was essentially the motivating argument[18,2] behind the n-$\bar{n}$ oscillation experiments. This is a compelling experiment from the viewpoint of its conceptual simplicity and model independent interpretation.

Although there have been strong advocates of proton decay, in analogy with beta decay, as a tool for exploring Grand Unification and the observed matter-antimatter asymmetry e.g. $p \to e^+\pi^\circ$ that conserves B-L, such decay channels appear unobservable.[19] Nevertheless, the limit on proton lifetime[20] $\tau \geq 10^{33}$ comes from this reaction. Other B-L conserved reactions are:

$$\begin{aligned} n &\to e^+\pi^- \\ n &\to \bar{\nu}\pi^\circ \\ np &\to \bar{\nu}e^+ \\ pp &\to l^+l^+ \end{aligned}$$

None of these have been observed[2] nor is there much prospect. For actual measurement, B-L nonconserving processes with reasonable energy scale[19] are:

$$\begin{aligned} n &\to e^-\pi^+ \\ n &\to e^-e^+\nu \\ n &\to \bar{n} \quad (\text{or } nn \to n\bar{n} \to X, \text{ annihilation}) \\ nn &\to ppe^-e^- \end{aligned}$$

Neutrinoless double beta decay is one of the more favorable. Although there are several ways to approach doing such experiments in this context, one intriguing possibility for n-n or n-$\bar{n}$ is colliding beams. However, rather than build two small systems one could consider using PEP-II i.e. the LER and HER rings to get the highest luminosity – as well as for the γ_1-γ_2 option ($\sqrt{s}_{\gamma\gamma} \leq 10$ keV).

12 Conclusions

A novel system for the production of neutron and gamma beams was discussed. Applications were considered for problems ranging in scale from the hardcore of the nucleon, through the Compton wavelength of the electron, to circuit feature sizes and the size of tumors in the brain to cosmological problems. Although a research project even at 200 MeV, the major problems were addressed here.

There were several reasons for choosing such a low energy: 1) the gain goes as $n_e(K\lambda_U)^2(N_U/\gamma)^3$, 2) the cost goes as γ and 3) efficiency e.g. lithography at 0.11 nm was consistent with neutron production at 1.7 MeV for BNCT or other uses. However, the 'difficulty' costs increase drastically with decreasing energy due to emittance dilution from intrabeam scattering. Because this goes inversely with the normalized phase volume[21] and the normalized emittances due to synchrotron radiation as $1/\gamma^3$, one expects the difficulty of reducing the energy to increase as $1/\gamma^{12}$ because conventional synchrotron damping goes as $1/\gamma^3$. One solution[3,22] to this, that goes as $1/\gamma$, was called 'fast damping'.

Tables of different machine characteristics were given elsewhere[3] including potential well distortion, microwave, transverse and longitudinal coupled bunch instabilities. Fast damping and the third order achromat (Fig. 2) were also considered there. A *practical* third order achromat was developed for large energy acceptance. Nevertheless, the limiting beam lifetimes resulted from diffusion due to intrabeam scattering on the restricted energy aperture that resulted from using conventional multipoles. The solution is a new combined function dipole[23]. Beyond a greatly improved energy aperture, it should be more compact, stable, less complex and improve the threshold for turbulent bunch lengthening. Our assumption of the mirror damage limit is consistent with counteracting bunch lengthening[7] i.e. being dominated by energy spread. This supposes no other problems such as strong-field, multiple scattering effects analogous to multiple Coulomb intrabeam scattering and its effects.

Because of space limitations, a more complete report on every aspect will be available[8] including a calculation with an improved lattice whose optics are based on the combined function magnet. A proper, self-consistent calculation is difficult but the one discussed in Ref 24 was extended to storage rings with undulators[24] to explicate some observed nonlinear resonances.

Acknowledgements
The author thanks Pisin Chen and the SLAC staff for a remarkable conference and Bill Bugg, Bob Byer, Roger Carr, Dan Porat, Alan Fisher, Ken Frankel, Bill Herrmannsfeldt, Albert Hofmann, Norman Kroll, James Liu, Phil Morton, W.K.H.(Pief) Panofsky, Tor Raubenheimer, Jerry Silverberg and Mort Weiss on various aspects of this work and especially Steve Shapiro for raising the original BNCT problem, with whom he has a pending patent (1/5/95).

References

1. The Eight Int'l. Symp. on Neutron Capture Therapy for Cancer, Sept.13-18, 1998, La Jolla, CA.
2. Future Prospects of Baryon Instability Search in P-Decay and n$\rightarrow\bar{n}$ Oscillation Experiments, ORNL-6910, Editors: S.J. Ball and Y.A. Kamyshkov, Oak Ridge, March 28-30, 1996.
3. P.L. Morton and J.E. Spencer, Design of an Efficient, Variable Energy, Variable Intensity Photon Beam, NSF Rept. under Contract 9560868, June 12, 1995.
4. L.L. Balakireeva, A. Vinogradov and I.V. Kozhevnikov, Optimization of High Reflectivity, Multilayer Mirrors for the Range of 100-150 nm, Kvantovaya Elektron. (Moscow), 20(No.9)(1993)933.
5. R.H. Helm, M.J. Lee, P.L. Morton and M. Sands, Evaluation of Synchrotron Radiation Integrals, *IEEE Trans. Nucl. Sci.* **20**, 900 (1973).
6. A. Hofmann, Synchrotron Radiation from the Large Electron-Positron

Storage Ring LEP, *Phys. Rept.* **64**, 253 (1980).
7. G. Dattoli, L. Mezi, A. Renieri, G.K. Voykov, Dynamics of a Storage Ring FEL Oscillator with Inclusion of Microwave Instability, *Nucl. Instrum. Methods* A **393**, 70 (1997).
8. J.E. Spencer, Efficient, High Brightness Sources of Polarized Neutrons and Photons and Their Uses, SLAC-PUB-7814, 1998.
9. H. Ohgaki, et al., Polarized gamma rays with laser-Compton backscattering, *Nucl. Instrum. Methods* A **375**, 602 (1996).They used a laser and 200-800 MeV ring TERAS. Also: V.N. Litvinenko, et al., Gamma-Ray Production in a Storage Ring FEL, *Phys. Rev. Lett.* **78**, 4569 (1997).
10. Large gains aren't possible without large damping losses but if the damping depends on the large gain then we need an external assist. Lasers are (commercially) available: M.H.Sher et al., 2 Hz 109-nm mirrorless laser, *Jrnl.Opt.Soc.Am. B*, **8**, 114 (1991). Because we can go to higher energies for more damping, more powerful lasers and better mirrors we will use this value for $\mathcal{N}_{\gamma 1}$. However, the importance of this particular frequency range strongly suggests that it will become available.
11. B.L. Berman, R.L. van Hemert and C.D. Bowman, Threshold Photoneutron Cross Section for Be^9, *Phys. Rev.* **163**, 958 (1967).
12. Robley D. Evans, *The Atomic Nucleus*, McGraw Hill, New York, 1955.
13. PEP-II Conceptual Design Report, SLAC-418, June 1993.
14. B.L. Berman, Photoneutron Cross Sections, *Atomic Data and Nuclear Data Tables*, 15, April 1975. For some reason the author did not include his own work[11] in this compilation.
15. J.A. Becker, J.D. Anderson, M.S. Weiss, Photoproduction of Tritium, UCRL-120596, 1995.
16. N.F. Ramsey, *Ann.Rev.Nucl.&Part.Sci.*, Edited by Jackson, Gove and Luth, Palo Alto, CA, Vol. 40, 1993.
17. See T. Plettner et al., These Proceedings and references therein.
18. R.E. Marshak and R.N. Mohapatra, *Phys. Lett.* B **91**, 2109 (1987).
19. Jogesh C. Pati, idem.
20. Pran Nath and R. Arnowitt, idem.
21. J.D.Bjorken, S.K.Mtinga, Intrabeam Scattering,*Part.Acc.***13**,115(1983).
22. For an essentially similar approach using lasers see: Z. Huang and R.D. Ruth, Laser-Electron Storage Ring, *Phys. Rev. Lett.* **80**, 976 (1998).
23. J.E. Spencer and H.A. Enge, Split-Pole Spectrograph for Precision Nuclear Spectroscopy, *Nucl. Instrum. Methods* **49**, 181 (1967). Also: Ring Enhancements Through Magnet Modifications, Proc. of DR2000, 1998.
24. J. Harris, P. Morton, J. Spencer and H. Winick, Undulator Induced Resonances, Proc. 12th Int'l. Conf. on High Energy Accel., 1983.